How to cite: *Angew. Chem. Int. Ed.* **2023,** *62,* e202212111
International Edition: doi.org/10.1002/anie.202212111
German Edition: doi.org/10.1002/ange.202212111

Proteomics **Hot Paper**

Profiling the Heme-Binding Proteomes of Bacteria Using Chemical Proteomics

*Isabel V. L. Wilkinson, Max Bottlinger, Yassmine El Harraoui, and Stephan A. Sieber**

Abstract: Heme is a cofactor with myriad roles and essential to almost all living organisms. Beyond classical gas transport and catalytic functions, heme is increasingly appreciated as a tightly controlled signalling molecule regulating protein expression. However, heme acquisition, biosynthesis and regulation is poorly understood beyond a few model organisms, and the heme-binding proteome has not been fully characterised in bacteria. Yet as heme homeostasis is critical for bacterial survival, heme-binding proteins are promising drug targets. Herein we report a chemical proteomics method for global profiling of heme-binding proteins in live cells for the first time. Employing a panel of heme-based clickable and photoaffinity probes enabled the profiling of 32–54 % of the known heme-binding proteomes in Gram-positive and Gram-negative bacteria. This simple-to-implement profiling strategy could be interchangeably applied to different cell types and systems and fuel future research into heme biology.

Introduction

Heme is an iron-coordinated protoporphyrin cofactor, which is essential to almost all living organisms. It is typically associated with proteins non-covalently (as heme *b*) or via covalent bonds between heme's vinyl groups and two cysteine thiols (as heme *c*). Heme performs a variety of functions, including transport, storage and metabolism of molecular oxygen and catalysis of electron transfer reactions. There is also growing appreciation of the role of heme in signal transduction through heme-responsive sensors which regulate multitudinous functions including transcription, DNA binding, miRNA biogenesis, translation, protein kinase activity, protein degradation, protein stabilisation, ion channel activity and many more.[1–4] The versatility of heme as a cofactor in part derives from its diverse protein scaffolds, which result in vastly varying binding affinities, ranging from less than pM for globin folds to ≈μM for heme chaperones or heme-regulated proteins.[5,6] Thus far, more than 30 different structural folds have been identified,[7] with new folds and potential therapeutic applications still being discovered.[8–10]

Pathogens require iron for growth and host colonisation, but free extracellular iron is limited as part of the human innate immune response.[11] Therefore, pathogens have evolved a range of methods to extract iron from the host, especially from heme and heme-binding proteins (HBPs) like hemoglobin.[12] Heme acquisition, biosynthesis and regulation is poorly understood beyond a few model organisms, and the heme-binding proteome has yet to be fully characterised in bacteria or humans.[13,14] However, heme acquisition and metabolism pathways have recently been identified as potential therapeutic targets against protozoan parasites,[15] *Mycobacterium tuberculosis*[16] and Gram-negative bacteria,[17] all of which have a high unmet need for novel drugs. Profiling the heme-binding proteome in bacteria is of great importance for understanding heme's role in infection and could also identify novel antibiotic targets.

Indeed, profiling of heme-binding proteomes has long been a research goal, with the greatest advancements emerging from computational prediction. These include tools to predict heme binding sites based on protein structure,[18] sequence[19–21] or both.[22,23] These tools are complemented by the more recently developed webserver HeMoQuest[24,25] which identifies residues that likely bind heme transiently. However, the high structural and functional diversity of heme-binding hinders in silico homology-dependent prediction. Moreover, in silico methods require experimental validation, for which unbiased global proteomics could offer a high-throughput solution.

To our knowledge, reported attempts to experimentally profile HBPs have thus far been confined to soluble lysates or extracts, typically by affinity chromatography using heme-conjugated agarose resins followed by SDS-PAGE (sodium dodecyl sulfate-polyacrylamide gel electrophoresis) and/or LC-MS/MS (liquid chromatography with tandem mass spectrometry) for identification of purified proteins.[26–32] This method has enabled the discovery of previously unknown heme-binding protein domains (such as for hERG3[27]), yet has some limitations: firstly, heme-conjugated resins may be sterically inhibited from accessing heme binding sites, or from being incorporated into heme *c* binding proteins. Furthermore, heme-conjugated resins

[*] I. V. L. Wilkinson, M. Bottlinger, Y. El Harraoui, S. A. Sieber
Centre for Functional Protein Assemblies, Technical University of Munich
Ernst-Otto-Fischer-Straße 8, 85748 Garching (Germany)
E-mail: stephan.sieber@tum.de

cannot be applied in living cells, may compete poorly for binding to HBPs already saturated with free heme, or fail to capture low affinity proteins. While this manuscript was in preparation, a report of chemical proteomic profiling of heme proteins in human cell lysates was published.[33] Applying a single heme-based photoaffinity probe, the authors isolate 19 proteins which are known to bind heme (≈10 % of total known hemoproteins[14]).

In summary, a method to specifically discover heme-binding proteins in live cells has yet to be reported, but would greatly contribute to the understanding of heme transport, metabolism and regulation. Herein we report a chemical proteomics method for global profiling of heme-binding proteins in situ which could be interchangeably applied to different cell types and systems. Application of the method enabled the profiling of 32–54 % of the known heme-binding proteomes in Gram-positive and Gram-negative bacteria, and revealed previously unknown potential heme interactors.

Results and Discussion

Chemoproteomics approaches to profiling protein binding partners of cofactors other than heme have been well-established and recently reviewed.[34] This work employs a similar strategy, beginning with the design and synthesis of heme probes to be metabolically incorporated into target live cells. These probes were designed to contain "click" reactive handles to allow for enrichment of the probe-HBP complex after target engagement. Enriched probe-bound HBPs can then be digested and the peptides identified by LC-MS/MS (Figure 1). In this work, the term 'heme' is used to refer to protoporphyrin IX containing either Fe^{II} or Fe^{III}.

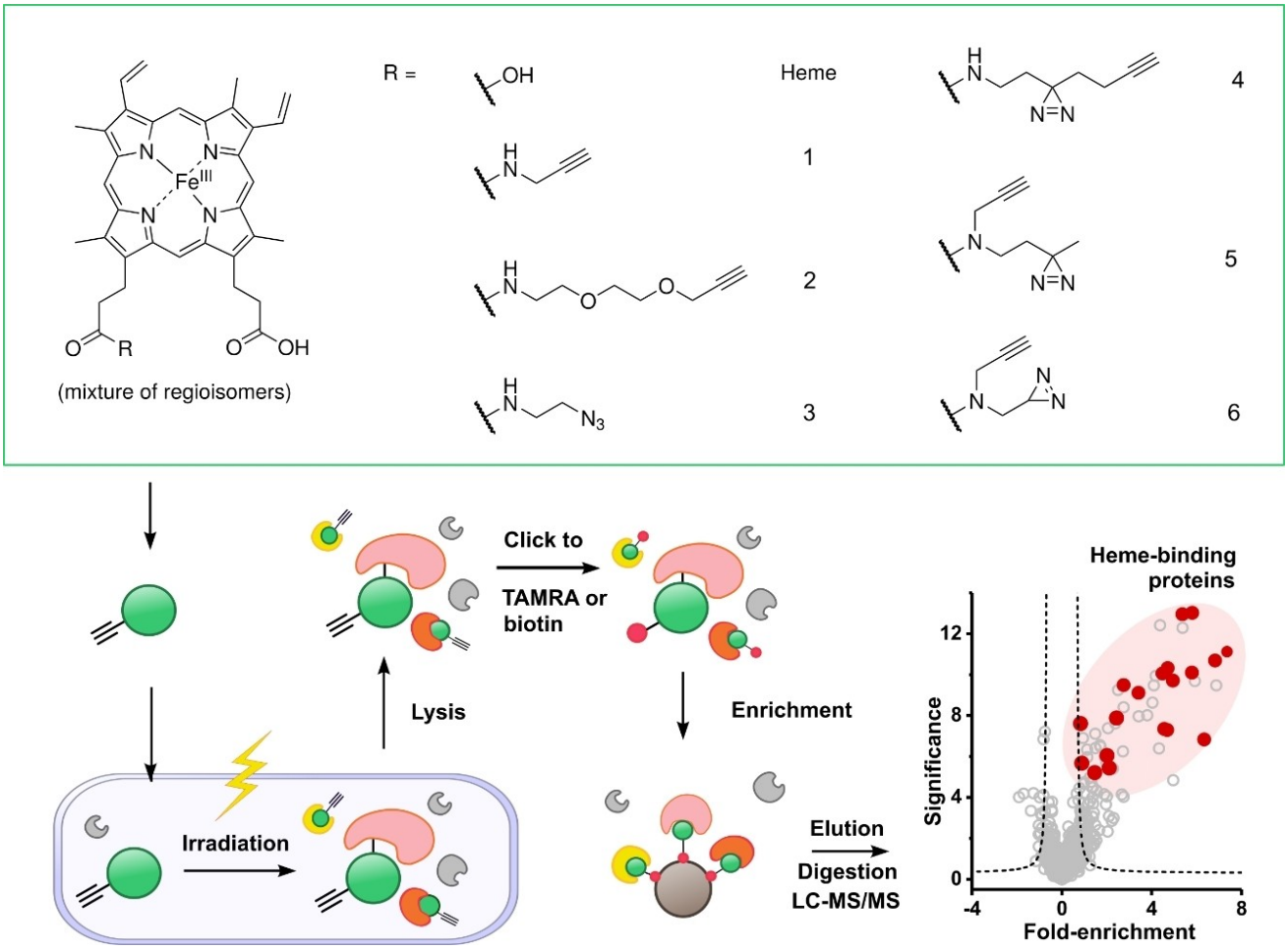

Figure 1. Structures of alkyne- and azide-bearing heme probes **1**–**3** and photoaffinity probes **4**–**6**, and schematic of the chemoproteomics strategy for profiling heme-binding proteins. Live cells are treated with a chosen heme probe, with photoaffinity probes irradiated (300 or 365 nm) to trigger covalent binding to adjacent biomolecules. Treated cells are lysed and probe-labelled cells ligated to biotin or TAMRA via copper-catalysed cycloaddition or Staudinger reaction. Fluorophore labelled samples are analysed by SDS-PAGE and in gel fluorescence while biotinylated samples are enriched on avidin beads. Enriched proteins are reduced, alkylated and digested and the resulting peptides desalted prior to analysis by liquid chromatography with tandem mass spectrometry (LC-MS/MS) for identification. SDS-PAGE: sodium dodecyl sulfate–polyacrylamide gel electrophoresis; TAMRA: tetramethylrhodamine.

The introduction of modifications should ideally minimally impact the ability of the probe to engage its cognate binding partners and phenocopy the original compound. Heme can interact with binding proteins through van der Waals and π–π stacking of its hydrophobic porphyrin ring, axial ligand coordination of the Fe ion (typically histidine, methionine, cysteine or tyrosine[7]), covalently to cysteine via its vinyl moieties or through hydrogen bonding or salt bridges to its propionate groups (usually through arginine[35]). Heme is typically significantly buried within a protein, but generally binds in a mode that exposes at least one propionate side chain to solvent.[36] For this reason, the propionate groups were chosen as the site for functionalisation for probe synthesis. Alkynes and azides were selected for their small size as the click handles, for tag ligation via bioorthogonal copper-catalysed cycloaddition or Staudinger reaction.[37]

Functionalisation of the protoporphyrin propionate groups through amide coupling[38–43] and subsequent reconstitution of example hemoproteins is well precedented.[44–48] In all cases, while double-reacted diamide products were separable from monoamides, the couplings were non-regioselective with respect to the two carboxylic acids, resulting in inseparable mixtures of monoamide regioisomers. In this work, monoamide Fe^{III} heme probes (**1**–**6**, Figure 1) were synthesised as regioisomer mixtures from hemin chloride (Fe^{III} protoporphyrin IX chloride) through amide coupling mediated by HBTU ((2-(1*H*-benzotriazol-1-yl)-1,1,3,3-tetramethyluronium hexafluorophosphate) and HOBt (hydroxybenzotriazole) (Scheme S1). Alongside the minimally sized propargylamide probe **1** and azide probe **3**, a polyethylene glycol (PEG)-linker containing alkyne probe **2** was also synthesised, to improve solubility and diversify accessibility of the alkyne for click ligation after binding of the probe to its target. The ability of these monoamide probes to reconstitute the activity of heme-bound horseradish peroxidase (HRP) was confirmed by in vitro assay using the apo-enzyme (Figure S1), indicating conservation of biological activity. By contrast, doubly-substituted dipropargylamide probe 7 (Figure S1) was incapable of reconstituting the activity of HRP.

Since the majority of HBPs bind heme non-covalently, the use of a photoaffinity heme probe, capable of UV-activatable covalent attachment to its target,[49] could greatly increase the number of proteins identified in these experiments. Incorporation of photoaffinity tags into probe structure without adversely affecting activity can be challenging, but has been expedited with the design of linear "minimalist" alkyne and diazirine containing photocrosslinkers by the Yao group.[50] Recently, the performance of linear, branched and terminal diazirine tags have been compared, finding that target enrichment can depend on the type of tag used, and that maximal identification of binding proteins may be best achieved through the parallel use of multiple photoaffinity tags.[51] Therefore, photoaffinity heme probes containing a linear, branched or terminal diazirine tag (probes **4**, **5**, **6** respectively, Figure 1) were also synthesised.

With a suite of six heme probes in hand, attention was turned to validation of their ability to phenocopy unmodified heme in a cellular context. Separation of the regioisomers of each probe **1**–**6** was not possible, however co-dosing of both monoamides together is anticipated to increase coverage of the heme-binding proteome that can be accessed, since for some heme-binding sites a particular propionate group (but not the other) is involved in protein binding.[36] Therefore, use of both isomers together would ideally only exclude from access those sites which require both propionate groups for binding.

Initial experiments were performed in the heme auxotroph Gram-positive bacterium *Enterococcus faecalis* (strain V583), a facultative anaerobe which is unable to biosynthesise heme but in the presence of exogenously supplied heme, switches on expression of heme-binding proteins.[52] *E. faecalis* V583 cells grown in TSBG medium (tryptic soy broth with 1 % glucose, containing < 0.05 μM heme[53]) were treated for 6 h in the exponential phase with alkyne-probe **1** (5 μM), hemin chloride (10 μM) or DMSO (dimethyl sulfoxide) vehicle (1 %) and the effects of treatment on the heme-binding proteome assessed by quantitative mass spectrometry (Figure 2a). Gratifyingly, heme-regulated transport efflux pump HrtBA[54] (EF_0792 and EF_0793), heme chaperone HemW (EF_1305) and cytochrome *bd* subunit CydA were clearly induced in the presence of either heme or heme probe **1**. Expression of heme transporter proteins CydDC[55,56] (EF_2058 and EF_2059) and non-canonical heme chaperones AhpC and Gap-2[57] was unaffected by heme treatment and likewise for heme probe **1**, while neither CydB nor newly reported heme transport regulator FhtR[54] were detected by mass spectrometry. However, expression of the heme-dependent catalase KatA[53] was induced only in the presence of heme and not heme probe **1**. Inspection of the reported KatA crystal structure[58] reveals the heme cofactor to be highly buried, with both propionate groups forming salt bridges with binding site arginine residues, thus rationalising the inability for monoamide **1** to bind in its place. The growth rate of *E. faecalis* V583 cells in TSBG medium supplemented with probe **1** was slower than with hemin, but reached the same maximum optical density at stationary phase (Figure S2a). Together, these results indicate the uptake and incorporation of probe **1** in live bacteria, in a similar manner to the unmodified heme. Expansion of the study to include probes **2**, **3** and **4** revealed the same effect on heme-binding protein expression as exhibited by probe **1** (Figure S3).

Next, we sought to evaluate the performance of the probes in *Pseudomonas aeruginosa*, a pathogenic Gram-negative bacterium with antibiotic resistant strains that have led to its designation as a WHO (World Health Organisation) priority pathogen.[59] *P. aeruginosa* encodes pathways to uptake heme directly and through the secreted hemophore HasAp.[17,60,61] The clinical importance of understanding heme acquisition has been highlighted by a study in cystic fibrosis patients showing that mutations developed in *P. aeruginosa* during host infection, which enabled scavenging of external heme as the sole source of iron, conferred growth advantages and contributed to chronic infection.[62]

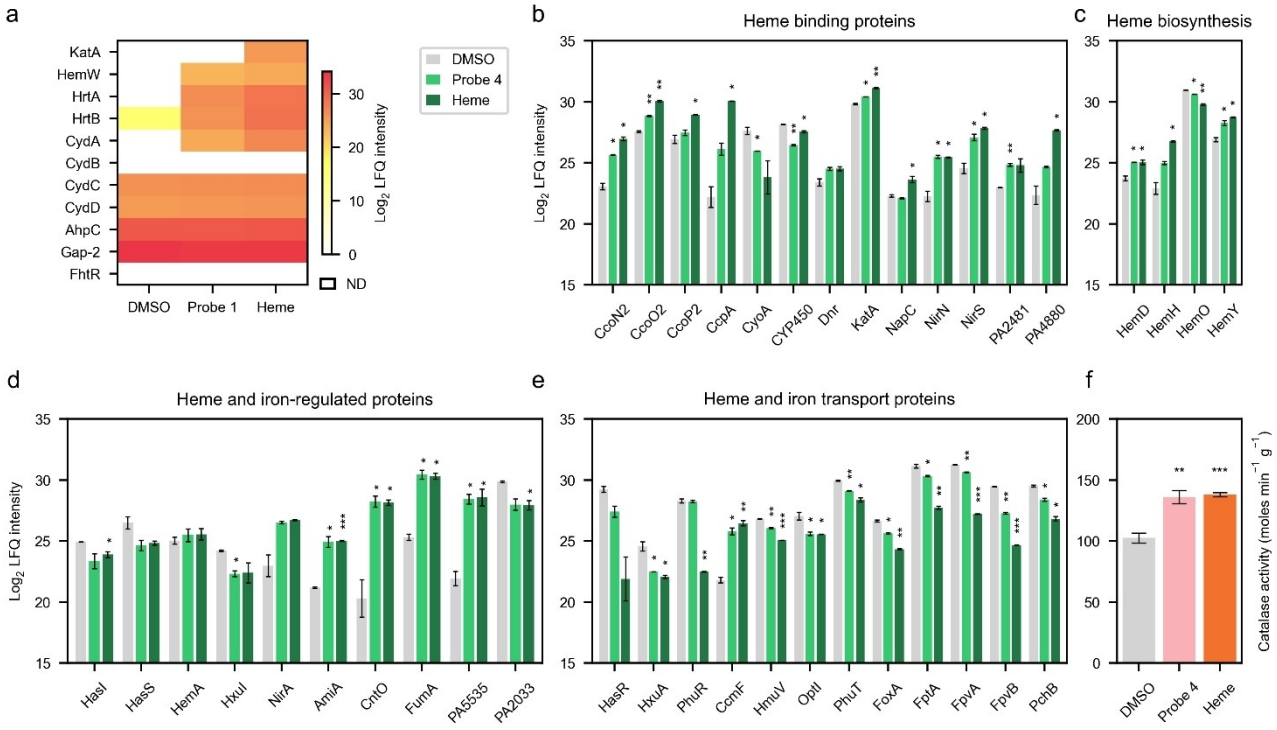

Figure 2. Validation of heme probes. a) heatmap of abundance of heme-binding proteins after 6 h treatment of *E. faecalis* V583 cells in the exponential phase with alkyne-probe **1** (5 μM), hemin chloride (10 μM) or DMSO vehicle (1 %); b) abundance of heme-binding proteins after 6 h treatment of *P. aeruginosa* PAO1 cells in stationary phase with photoaffinity probe **4** (5 μM) or heme (5 μM); c) abundance of heme biosynthesis proteins after 6 h treatment of PAO1 cells in exponential phase with photoaffinity probe **4**; d) abundance of heme- and iron-regulated proteins (HasI to NirA and AmiA to PA2033 respectively) after 1 h treatment of PAO1 cells in exponential phase with photoaffinity probe **4**; e) abundance of heme- and iron-transport proteins (HasR to PhuT and FoxA to PA4514 respectively) after 6 h treatment of PAO1 cells in exponential phase with photoaffinity probe **4**; f) catalase activity per gram of PAO1 lysate generated from cells treated in the exponential phase for 6 h with DMSO, **4** (5 μM) or hemin chloride (5 μM). DMSO: dimethyl sulfoxide; LFQ: label-free quantification; ND: not detected; all error bars represent standard deviation; stars denote significance as calculated by *t*-test: * $p < 0.05$, ** $p < 0.005$, *** $p < 0.0005$.

P. aeruginosa PAO1 cells grown in a chemically defined minimal medium lacking iron and heme were treated for 1 or 6 h in the exponential phase, or 6 h in the stationary phase with either photoaffinity probe **4** (5 μM), hemin chloride (5 μM) or DMSO vehicle (1 %) and the effects of treatment on the proteome assessed by quantitative mass spectrometry. In general, changes in protein expression induced by heme treatment were also observed with heme probe treatment. For example, cytochrome c proteins CcoN2, CcoO2, CcoP2, CcpA, NirS and PA2481[60] (which bind heme covalently) are upregulated in both conditions (Figure 2b), likewise for heme biosynthesis proteins HemD, HemH and HemY (Figure 2c) and iron-regulated proteins[63] AmiA, CntO, FumA (PA4333) and PA5535 (Figure 2d). However, TonB heme transporters HasR, HxuA and PhuR are downregulated in the presence of heme at 5 μM (higher than the typical availability of heme in eukaryotic cells, estimated to be between 0.025 and 0.3 μM[64]), but only HasR and HxuA were concomitantly downregulated by photoaffinity probe **4**. Ferri-siderophore transporters, such as FoxA, FptA, FpvA and FpvB have been previously reported to be downregulated in the presence of exogenous heme, enabling adaptation to prioritise iron acquisition through heme rather than iron uptake pathways.[60] Accordingly, in this work, these transporters were found to be significantly downregulated by treatment with either heme or heme-based photoaffinity probe **4** (Figure 2e). Furthermore, upregulation of catalase KatA expression and increased catalase activity were both observed with heme and heme probe treatment (Figure 2b,f). Finally, supplementation of chemically defined minimal media with heme, probe **1** or probe **4** each promoted growth of PAO1 cells compared to vehicle control (Figure S2b).

Having demonstrated the ability of amide-functionalised heme probes to substitute for heme in example Gram-positive and negative species, attention was turned to enrichment of heme-binding proteins from live cells. *E. faecalis* V583 cells grown to stationary phase in TSBG medium were treated with probe **1**, **2** or **3** (5 μM) with and without heme (10 μM) or DMSO vehicle (1 %) for 1 h (37 °C, 200 rpm). Excess probe was removed by washing, and after lysis, labelled proteins were clicked to tetramethylrhodamine (TAMRA) (Figure S4) or biotin for enrichment with streptavidin beads. 5 heme-binding proteins (45 %) were detected by quantitative mass spectrometry as two-fold enriched over control (Figure 3a, Table S1 lists to date known *E. faecalis* V583 heme-binding proteins).

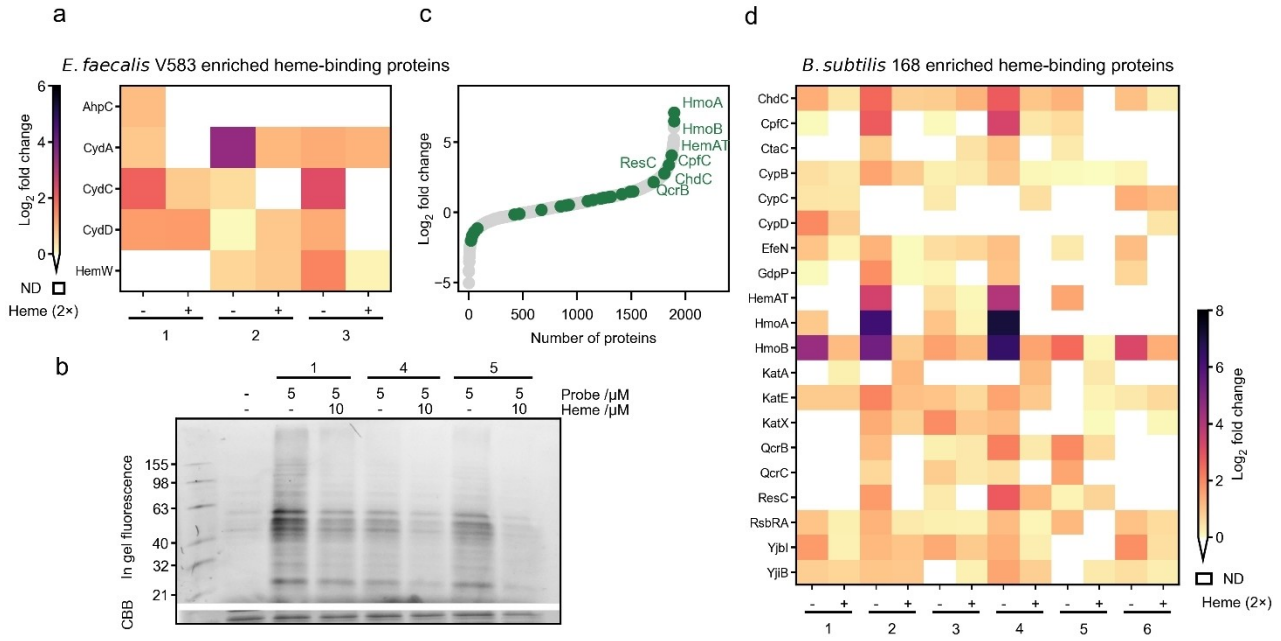

Figure 3. Profiling of heme-binding proteins in Gram-positive strains *E. faecalis* V583 (a heme auxotroph) and *B. subtilis* 168. a) Heatmap of heme-binding proteins enriched by probes **1**, **2** and **3** (5 μM) over co-treatment with heme (+, 10 μM) or DMSO vehicle control (−, 1%) in live *E. faecalis* V583 cells. Only proteins two-fold enriched by at least one probe are shown; b) Profiling of heme-binding proteins in *B. subtilis* 168 using probes **1**, **4** and **5** (5 μM). TAMRA-treated samples were separated by SDS-PAGE, and labelled proteins visualised by in gel fluorescence. Total protein content was visualised using Coomassie Brilliant Blue (CBB); c) waterfall plot of proteins enriched by alkyne-probe **1** (5 μM) over DMSO vehicle control (1%) in live *B. subtilis* strain 168 cells, green: heme-binding proteins, of which those meeting criteria $\log_2$ fold change >2 and $p<0.05$ are labelled; d) heatmap of heme-binding proteins enriched by probes **1**–**6** (5 μM) over co-treatment with heme (+, 10 μM) or DMSO vehicle control (−, 1%) in live *B. subtilis* strain 168 cells. Only proteins two-fold enriched by at least one probe are shown. ND: not detected; SDS-PAGE: sodium dodecyl sulfate–polyacrylamide gel electrophoresis; TAMRA: tetramethylrhodamine.

Building on this proof of principle in *E. faecalis* V583 cells, the same methodology was applied to the Gram-positive model organism *B. subtilis*, which can utilise exogenous heme for cytochrome c synthesis[65] and to overcome the loss of heme biosynthesis in a *HemA* mutant.[66] Treatment of *B. subtilis* (strain 168) with probe **1**, **4** or **5** (5 μM) with and without heme (10 μM), or DMSO vehicle (1%), for 1 h (37 °C, 200 rpm) followed by irradiation (5 min, 365 nm) for the photoaffinity probes and click to TAMRA led to probe-dependent labelling which was competed in the presence of the 2-fold excess of heme (Figure 3b). Profiling with all six heme probes led to the identification of 20 heme-binding proteins (Figure 3d, Table S2 lists to date known *B. subtilis* (strain 168) heme-binding proteins (recently reviewed[67])), with heme monooxygenases HmoA and HmoB as the top hits (Figure 3c). Interestingly, a large number of reversibly binding heme proteins were also enriched by probes lacking a photocrosslinker, suggesting that proteins with a tightly bound cofactor are stable throughout the sample preparation. This is in line with previous reports of unfolded heme *b*-binding polypeptides retaining interactions with their heme cofactor.[68–70]

Profiling the heme binding proteomes of Gram-negative strains was the next focus. First, *P. aeruginosa* PAO1 cells grown in LB medium to stationary phase were resuspended in chemically defined minimal medium and treated with probes **1**–**6** (5 μM) with and without heme (10 μM) or DMSO vehicle (1%) for 1 h (37 °C, 200 rpm), followed by irradiation (5 min, 365 nm for alkyl diazirine probes **4** and **5** or 300 nm for the terminal diazirine probe **6**, and accompanying DMSO controls). After lysis, click to biotin, and enrichment with streptavidin beads, numerous heme-binding proteins were found to be selectively enriched by the probes, and displaced in the presence of two-fold excess of heme, an indication of heme-specific binding (Figures 4a,b,f, Table S3 lists to date known *P. aeruginosa* PAO1 heme-binding proteins). Gene ontology analysis[71] of the molecular functions of proteins bound by the heme-probes but competed in the presence of excess heme revealed enrichment of heme-related functions such as cytochrome c peroxidase and oxidase activity, heme binding and oxidoreductase activity (e.g. Figure 4d for probe **3**).

Heme proteome profiling was also investigated using photoaffinity probe **4** under different conditions, such as during the exponential phase, after 4 h nutrient starvation, and after growth solely in chemically defined minimal media (Figure 4c), as growth stage and nutrient availability are known to influence protein expression,[60,63,72–74] and could therefore enable the identification of heme-binding proteins which were previously undetectable. Across the suite of six probes and seven different labelling conditions, a total of 57 different PAO1 heme-binding proteins were identified (Figure 4f). Some, such as heme oxygenase HemO and heme

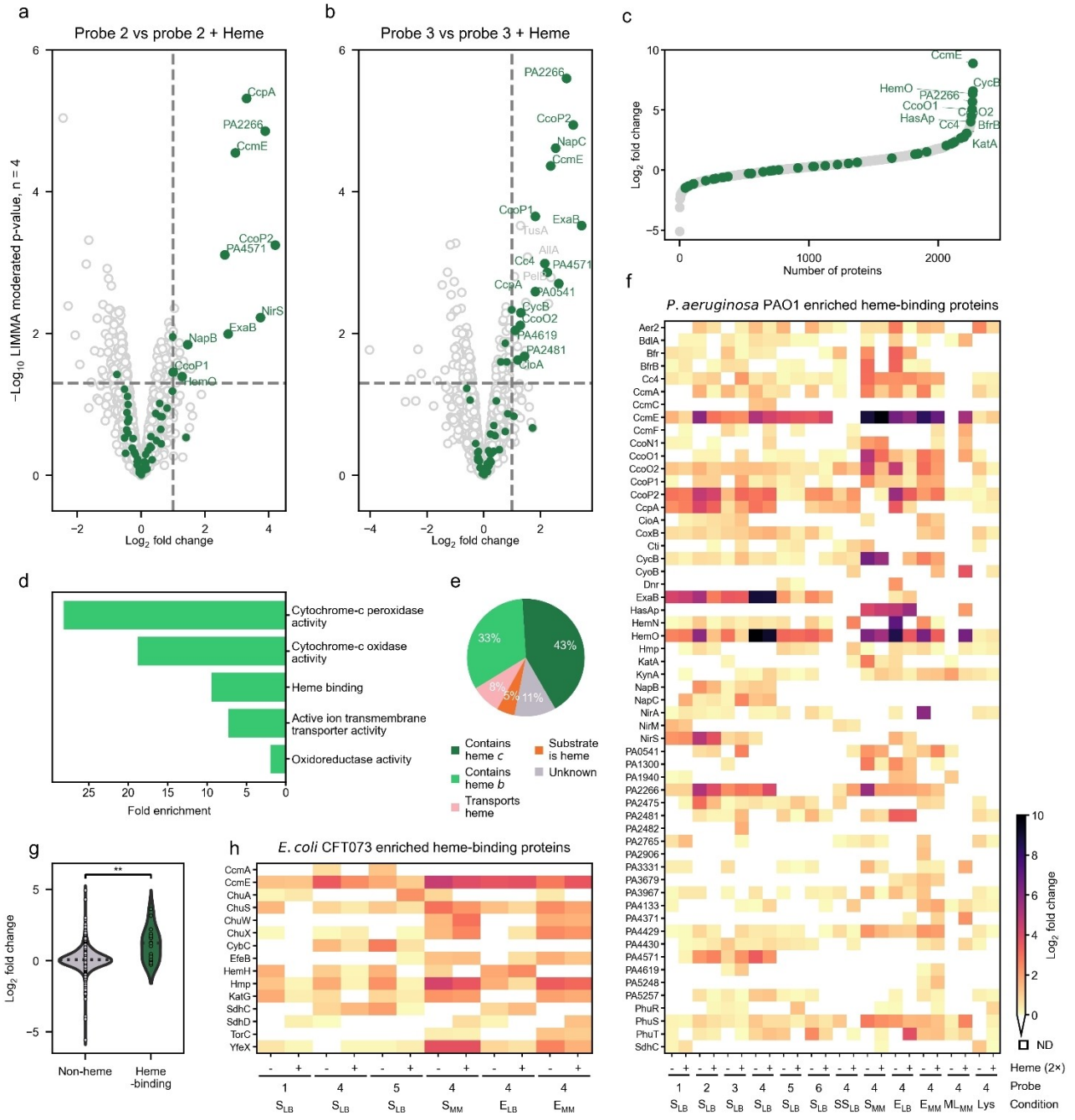

Figure 4. Profiling of heme-binding proteins in Gram-negative strains *P. aeruginosa* PAO1 and *E. coli* CFT073. Volcano plots of proteins enriched by alkyne-probe **2** (a, 5 μM) or azide-probe **3** (b, 5 μM) in live PAO1 cells. Green dots: heme-binding proteins, thresholds: $\log_2$ fold change >1 and $p<0.05$. Fold change and significance of protein enrichment upon probe treatment vs. co-treatment with heme (2-fold excess) were calculated using a LIMMA-moderated *t*-test (implemented in R); c) waterfall plot of proteins enriched by photoaffinity probe 4 (5 μM) over DMSO vehicle control (1%) in live PAO1 cells, green: heme-binding proteins, of which those meeting criteria $\log_2$ fold change >2.75 and $p<0.05$ are labelled; d) Gene ontology analysis[71] of molecular functions enriched in proteins with $\log_2$ fold change >1 from volcano plot (b); e) pie chart of total heme-binding proteins two-fold enriched from PAO1, sorted by mode of heme-binding, listed breakdown given in Table S5; f) heatmap of heme-binding proteins enriched by probes **1**–**6** (5 μM) over co-treatment with heme (+, 10 μM) or DMSO vehicle control (−, 1%) in live PAO1 cells. Only proteins two-fold enriched by at least one probe are shown. Condition subscript denotes medium the cells were grown in; treatments were performed in chemically defined minimal medium; g) violin plot of proteins enriched by photoaffinity probe **4** in *E. coli* CFT073 cells shows significant enrichment of heme-binding proteins, $p=0.00465$ determined using Welch's *t*-test; h) heatmap of heme-binding proteins enriched by probes **1**, **4** and **5** (5 μM) over co-treatment with heme (+, 10 μM) or DMSO vehicle control (−, 1%) in live *E. coli* CFT073 cells. Only proteins two-fold enriched by at least one probe are shown, colour bar and labels shared with (f). Condition subscript denotes medium the cells were grown in; treatments were performed in chemically defined minimal medium. E: exponential phase labelling; ML: metabolic labelling; LIMMA: Linear Model to Microrray Data; Lys: lysate labelling; ND: not detected; S: stationary phase labelling; SS: starved stationary phase labelling.

chaperone CcmE were highly and selectively enriched across multiple probes and conditions, whereas others, such as nitrite reductase NirS and probable cytochrome c PA4571 were only identified in a subset of conditions, highlighting the need for diverse probes and profiling conditions to maximise heme profiling coverage. Additionally, heme proteome profiling was also performed in cell lysates, which resulted in a marked reduction in enrichment of heme-binding proteins compared to profiling in live cells (Figure 4f), thus underlining the benefits of our in situ profiling strategy. Analysis of the identified heme-binding proteins showed that both proteins binding heme covalently (contain heme *c*, 43 % of the total identified) and non-covalently can be readily accessed with our heme-probes (Figure 4e).

Finally, heme proteome profiling was performed in the uropathogenic *Escherichia coli* strain CFT073, which expresses TonB-dependent heme transporters ChuA and Hma (c2482) that are required for virulence in mice.[75,76] In CFT073 cells grown in chemically defined minimal medium and treated for 1 h in the exponential phase (condition E_{MM}, photoaffinity probe **4**, 5 μM), total heme-binding proteins were significantly enriched over non-heme proteins ($p = 0.00465$, Figure 4g, Table S4 lists to date known *E. coli* strain CFT073 heme-binding proteins). Across probes **1**, **4** and **5** and four different labelling conditions in live cells, 15 heme-binding proteins were accessed, including heme enzymes (ChuS, EfeB, HemH, Hmp, SdhC, YfeX), transporters (ChuA) and chaperones (CcmE) (Figure 4h).

An advantage of global, unbiased experimental profiling is the ability to identify previously unannotated, potential heme interactors or to confirm computational predictions. For example, the *P. aeruginosa* PAS1 domain containing redox-responsive sensor kinase MxtR (PA3271)[77] was recently predicted to bind heme through sequence alignment,[78] and was here found to be two-fold enriched by photoaffinity probe **6** (Figure 5a, $p = 0.039$). Filtering the data for proteins previously unannotated as heme-binders and enriched at least 3-fold over DMSO and heme competitor controls in at least two conditions gave a list of potential heme interactors for each species (Figure 5b, breakdown of enrichment per condition in Figure S5). Since these shortlisted proteins each lacked the canonical CXXCH sequence indicating binding of heme *c*, the HeMoQuest webserver[25] was employed to identify transient heme-binding motifs using its SeqD-HBM[24] algorithm. This tool also predicts the heme-binding affinities of the individual motifs using a machine learning approach trained on experimental data, and sites with predicted affinity < 3 μM are listed in Figure 5b. Among these shortlisted proteins are many uncharacterised proteins, but also plausible heme-binders based on their known functions, such as the *B. subtilis* 168 putative oxidoreductase YxnA or putative PAO1 iron utilisation protein PA2033 which also has oxidoreductase annotation.

To validate heme binding to identified hits we exemplarily selected three proteins for recombinant expression and

a

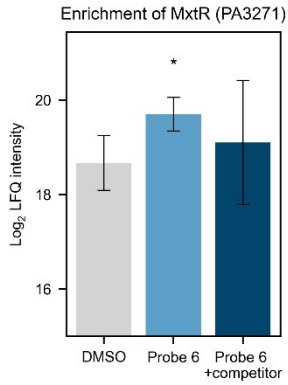

b

Organism	Uniprot	Gene	Description	HeMoQuest predicted binding residues
P. aeruginosa PAO1	Q9HT86	AmpDh2	Zinc protease, virulence determinant	C17, H86, H153
	Q9HZW2	AtuR	Putative repressor of atu genes	H26, H54, C98
	Q9I115	FoxR	Anti-sigma factor	H18, Y275, H318
	Q9HXJ1	HscB	Co-chaperone protein	H6, H35, Y73
	Q9I777	PA0055	Uncharacterized protein	H30, H154
	Q9I4H7	PA1160	Uncharacterized protein	C41, H47, H85, C94
	Q9I282	PA2033	FAD-binding FR-type domain-containing protein	Y6, H114, H147, H200
	Q9HVV0	PA4469	Uncharacterized protein	H79, Y107, H149
	Q9HV30	PA4778	Uncharacterized HTH-type transcriptional regulator	Y36, H38, C120
	Q9HTY2	PA5208	Uncharacterized protein	H21, H71
	Q9I184	PvdF	Pyoverdine synthetase F	Y110, H120, H132
	Q9I3F3	TusA	Sulfur carrier protein	C16 (CP motif), C53
E. coli CFT073	A0A0H2V8M3	C2463	Putative transacylase	C49, H88, C168, C410
	A0A0H2V868	FocH	F1C Putative fimbrial adhesin	H7, Y184, C217
	P63021	NfuA	Fe/S biogenesis protein	H126, C149, H188
	A0A0H2VE59	RbsB	D-ribose-binding periplasmic protein	Y142, H179
	A0A0H2V7R8	Spy	Spheroplast protein Y	H40, H88
	Q8FKZ8	YaeP	UPF0253 protein	C5, C29
	A0A0H2VAY6	YqiC	Ubiquinone biosynthesis accessory factor UbiK	Y5, H35
E. faecalis V583	Q838Y4	CopZ	Copper transport protein	C15
	Q839C3	EF_0252	N-acetylmuramoyl-L-alanine amidase, family 4	H319, H347, C395
	H7C7B7	EF_3129	D-alanyl-D-alanine carboxypeptidase	C26, H461
	Q82YP8	EF_C0011	Transcriptional regulator, UvrC family	H9, C52, H54
B. subtilis 168	P37469	DnaC	Replicative DNA helicase	H177, C253
	P40872	PksM	Polyketide synthase	H272, H522, H762, H3416
	O31606	SpxH	ClpXP adapter protein	H14, H72, H165
	O32291	YxnA	Uncharacterized oxidoreductase	H255, H314

Figure 5. Chemical proteomics profiling reveals potential heme interactors. a) Enrichment of sensor kinase MxtR (PA3271), recently predicted to bind heme, by terminal diazirine probe **6**, $p = 0.039$. Error bars represent standard deviation; b) table of top enriched, previously unannotated, potential heme interactor proteins ($p < 0.05$, breakdown of enrichment per condition in Figure S5). Prediction of heme-binding residues performed using the HeMoQuest webserver,[25] residues with predicted binding affinity $\lesssim 3$ μM shown. LFQ: label-free quantification.

labelling. Heme oxygenase HmoB from *B. subilis* served as positive control along with two proteins Spy (*E. coli*) and PA2033 (*P. aeruginosa*) which were previously unknown to bind heme. Satisfyingly, all proteins showed labelling with heme probe **4** as well as concentration-dependent competition with free heme, confirming the fidelity of our approach (Figure S6).

Conclusion

In pursuit of a chemical proteomics strategy for the profiling of heme-binding proteins, six heme-based probes were synthesised through amide functionalisation of one of heme's two propionate sidechains. Amongst these six were three diazirine-containing photoaffinity probes. Comparative proteomics studies indicated the uptake and incorporation of the heme probes in example live Gram-positive and -negative bacteria in a similar manner to unmodified heme, in heme auxotroph and non-auxotroph bacteria alike. These probes were then applied to enrich and identify heme-binding proteins from live *E. faecalis* V583, *B. subtilis* 168, *P. aeruginosa* PAO1 and *E. coli* strain CFT073 cells (Figure 6a). This methodology enabled enrichment of heme-binding proteins diverse in function and mode of heme-binding (Figure 4d,e) while also enriching homologues across the investigated species for example, heme chaperones (CcmE or PhuS/ChuS), heme enzymes (Hmp, SdhC or EfeB/EfeN), heme receptors (PhuR/ChuA) and transporters (CcmA/CydD) (Figure 6b, Table S6). The combination of multiple probes and various growth conditions was required to increase the coverage of enriched heme-binding proteins. Thus, in this work 32–54 % of the total heme-binding proteomes were enriched in the four different bacterial species (Figure 6c) using an easily adaptable and simple-to-implement experimental setup. Of the known heme-binding proteins which were not enriched by this strategy, significant proportions were not detected at all by mass spectrometry (Figure 6c). Improvement to the coverage of heme-binding proteome profiling for a particular target species may be achieved through optimisation of labelling conditions or use of methods to increase the depth of proteome coverage.[79–81]

This method for global characterisation of heme-binding proteomes in live cells represents a technological advance over all previous reports, and could be readily adapted for use in other target cell types which uptake heme, including pathogens such as *Staphylococcus aureus*,[83] *Listeria monocytogenes*[84] or *Aspergillus* species,[85] or heme auxotrophs such as *Haemophilus influenzae*,[86] *Streptococcus pneumoniae*,[87,88] marine microbes[89] or *Caenorhabditis elegans*.[90] Since dysregulation of heme transport and regulation reduces bacterial pathogenicity and heme homeostasis is critical for bacterial survival, heme-binding proteins are promising drug targets.[3,12] Profiling of heme binding proteins could therefore enable the identification of novel

a

Organism	Probes applied	Known heme-binding proteins enriched	Previously unknown potential heme binders enriched
P. aeruginosa PAO1	1, 2, 3, 4, 5, 6	57	12
B. subtilis 168	1, 2, 3, 4, 5, 6	20	4
E. faecalis V583	1, 2, 3	5	4
E. coli CFT073	1, 4, 5	15	7

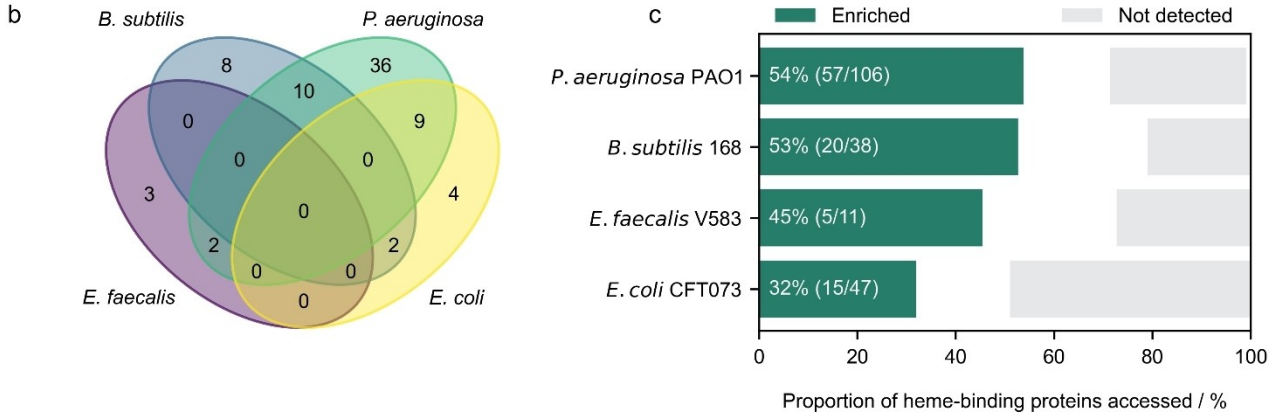

Figure 6. Summary of heme-binding proteome profiling achieved in this work. a) Summary table of the organisms investigated and the probes applied; b) Venn diagram of heme-binding proteins enriched in this study, identified homologues (determined using Blastp[82] as sequences with significant alignment) are placed in the intersections. All homologues are listed in Table S6; c) proportion of heme-binding proteins accessed in this work in the four investigated strains.

antibiotic targets as well as provide valuable insights into heme regulation and biology.

Acknowledgements

I.V.L. Wilkinson would like to thank the European Molecular Biology Organisation for financial support (ALTF 484-2020). Y.E.H thanks Till Reinhardt for internship supervision. SAS acknowledges the European Research Council (ERC) and the European Union's Horizon 2020 research and innovation program (grant agreement no. 725085, CHEMMINE, ERC consolidator grant). Open Access funding enabled and organized by Projekt DEAL.

Conflict of Interest

The authors declare no conflict of interest.

Data Availability Statement

The proteomics data have been deposited to the ProteomeXchange Consortium[91] via the PRIDE[92] partner repository. Data are available via ProteomeXchange with identifier PXD036133.

Keywords: Chemical Probes · Cofactors · Heme Proteins · Photoaffinity Labelling · Proteomics

[1] H. M. Girvan, A. W. Munro, *J. Biol. Chem.* **2013**, *288*, 13194–203.
[2] T. Shimizu, A. Lengalova, V. Martínek, M. Martínková, *Chem. Soc. Rev.* **2019**, *48*, 5624–5657.
[3] H. H. Brewitz, G. Hagelueken, D. Imhof, *Biochim. Biophys. Acta Gen. Subj.* **2017**, *1861*, 683–697.
[4] T. Shimizu, D. Huang, F. Yan, M. Stranava, M. Bartosova, V. Fojtíková, M. Martínková, *Chem. Rev.* **2015**, *115*, 6491–6533.
[5] X. Yuan, N. Rietzschel, H. Kwon, A. B. W. Nuno, D. A. Hanna, J. D. Phillips, E. L. Raven, A. R. Reddi, I. Hamza, *Proc. Natl. Acad. Sci. USA* **2016**, *113*, E5144–E5152.
[6] A. E. Gallio, S. S.-P. Fung, A. Cammack-Najera, A. J. Hudson, E. L. Raven, *JACS Au* **2021**, *1*, 1541–1555.
[7] T. Li, H. L. Bonkovsky, J. Guo, *BMC Struct. Biol.* **2011**, *11*, 13.
[8] R. D. Latham, M. Torrado, B. Atto, J. L. Walshe, R. Wilson, J. M. Guss, J. P. Mackay, S. Tristram, D. A. Gell, *Mol. Microbiol.* **2020**, *113*, 381–398.
[9] S. Che, Y. Liang, Y. Chen, W. Wu, R. Liu, Q. Zhang, M. Bartlam, *FEBS J.* **2022**, *289*, 1911–1928.
[10] D. Khan, D. Lee, G. Gulten, A. Aggarwal, J. Wofford, I. Krieger, A. Tripathi, J. W. Patrick, D. M. Eckert, A. Laganowsky, J. Sacchettini, P. Lindahl, V. A. Bankaitis, *eLife* **2020**, *9*, e57081.
[11] C. C. Murdoch, E. P. Skaar, *Nat. Rev. Microbiol.* **2022**, *20*, 657–670.
[12] J. E. Choby, E. P. Skaar, *J. Mol. Biol.* **2016**, *428*, 3408–28.
[13] A. D. Smith, A. Wilks, *Current Topics in Membranes*, Academic Press, New York, **2012**, pp. 359–392.
[14] C. Andreini, V. Putignano, A. Rosato, L. Banci, *Metallomics* **2018**, *10*, 1223–1231.
[15] G. C. Lechuga, M. C. S. Pereira, S. C. Bourguignon, *J. Drug Targeting* **2019**, *27*, 767–779.
[16] A. Mitra, Y.-H. Ko, G. Cingolani, M. Niederweis, *Nat. Commun.* **2019**, *10*, 4260.
[17] K. L. Richard, B. R. Kelley, J. G. Johnson, *Front. Cell. Infect. Microbiol.* **2019**, *9*, 81.
[18] R. Liu, J. Hu, *PLoS One* **2011**, *6*, e25560.
[19] Y. Xiong, J. Liu, W. Zhang, T. Zeng, *Proteome Sci.* **2012**, *10*, S20.
[20] D. J. Yu, J. Hu, J. Yang, H. Bin Shen, J. Tang, J. Y. Yang, *IEEE/ACM Trans. Comput. Biol. Bioinf.* **2013**, *10*, 994–1008.
[21] Y. F. Liou, P. Charoenkwan, Y. Srinivasulu, T. Vasylenko, S.-C. Lai, H.-C. Lee, Y.-H. Chen, H.-L. Huang, S.-Y. Ho, *BMC Bioinf.* **2014**, *15*, S4.
[22] J. Zhang, H. Chai, B. Gao, G. Yang, Z. Ma, *IEEE/ACM Trans. Comput. Biol. Bioinf.* **2018**, *15*, 147–156.
[23] R. Liu, J. Hu, *BMC Bioinf.* **2011**, *12*, 207.
[24] A. Wißbrock, A. A. P. George, H. H. Brewitz, T. Kühl, D. Imhof, *Biosci. Rep.* **2019**, *39*, 20181940.
[25] A. A. Paul George, M. Lacerda, B. F. Syllwasschy, M. T. Hopp, A. Wißbrock, D. Imhof, *BMC Bioinf.* **2020**, *21*, 124.
[26] N. Wang, J. Zhang, L. Zhang, X.-Y. Yang, N. Li, G. Yu, J. Han, K. Cao, Z. Guo, X. Sun, Q.-Y. He, *Metallomics* **2014**, *6*, 1451.
[27] M. J. Burton, J. Cresser-Brown, M. Thomas, N. Portolano, J. Basran, S. L. Freeman, H. Kwon, A. R. Bottrill, M. J. Llansola-Portoles, A. A. Pascal, R. Jukes-Jones, T. Chernova, R. Schmid, N. W. Davies, N. M. Storey, P. Dorlet, P. C. E. Moody, J. S. Mitcheson, E. L. Raven, *J. Biol. Chem.* **2020**, *295*, 13277–13286.
[28] M. Azuma, Y. Kabe, C. Kuramori, M. Kondo, Y. Yamaguchi, H. Handa, *PLoS One* **2008**, *3*, e3070.
[29] B. R. Otto, S. J. M. Van Dooren, J. H. Nuijens, J. Luirink, B. Oudega, *J. Exp. Med.* **1998**, *188*, 1091–1103.
[30] B. C. Lee, *Infect. Immun.* **1992**, *60*, 810–816.
[31] X. Li, X. Wang, K. Zhao, Z. Zhou, C. Zhao, R. Yan, L. Lin, T. Lei, J. Yin, R. Wang, X. Feng, S. Liu, *Genomics Proteomics Bioinf.* **2003**, *1*, 78–86.
[32] V. C. Tsolaki, S. K. Georgiou-Siafis, A. I. Tsamadou, S. A. Tsiftsoglou, M. Samiotaki, G. Panayotou, A. S. Tsiftsoglou, *J. Cell. Physiol.* **2022**, *237*, 1315–1340.
[33] R. A. Homan, A. M. Jadhav, L. P. Conway, C. G. Parker, *J. Am. Chem. Soc.* **2022**, *144*, 15013–15019.
[34] I. V. L. Wilkinson, M. Pfanzelt, S. A. Sieber, *Angew. Chem. Int. Ed.* **2022**, *61*, e202201136; *Angew. Chem.* **2022**, *134*, e202201136.
[35] S. Schneider, J. Marles-Wright, K. H. Sharp, M. Paoli, *Nat. Prod. Rep.* **2007**, *24*, 621–630.
[36] L. J. Smith, A. Kahraman, J. M. Thornton, *Proteins Struct. Funct. Bioinf.* **2010**, *78*, 2349–2368.
[37] C. G. Parker, M. R. Pratt, *Cell* **2020**, *180*, 605–632.
[38] I. C. Reynhout, J. J. L. M. Cornelissen, R. J. M. Nolte, *J. Am. Chem. Soc.* **2007**, *129*, 2327–2332.
[39] A. Amirshaghaghi, B. Altun, K. Nwe, L. Yan, J. M. Stein, Z. Cheng, A. Tsourkas, *J. Am. Chem. Soc.* **2018**, *140*, 13550–13553.
[40] F. Liu, A. Soh Yan Ni, Y. Lim, H. Mohanram, S. Bhattacharjya, B. Xing, *Bioconjugate Chem.* **2012**, *23*, 1639–1647.
[41] A. Nakagawa, N. Ohmichi, T. Komatsu, E. Tsuchida, *Org. Biomol. Chem.* **2004**, *2*, 3108–3112.
[42] I. Hamachi, K. Nakamura, A. Fujita, T. Kunitake, *J. Am. Chem. Soc.* **1993**, *115*, 4966–4970.
[43] E. Monzani, L. Linati, L. Casella, L. De Gioia, M. Favretto, M. Gullotti, F. Chillemi, *Inorg. Chim. Acta* **1998**, *273*, 339–345.
[44] J. J. Woodward, N. I. Martin, M. A. Marletta, *Nat. Methods* **2007**, *4*, 43–45.

[45] I. Hamachi, S. Tanaka, S. Tsukiji, S. Shinkai, S. Oishi, *Inorg. Chem.* **1998**, *37*, 4380–4388.
[46] T. Matsuo, T. Hayashi, Y. Hisaeda, *J. Am. Chem. Soc.* **2002**, *124*, 11234–11235.
[47] K. Oohora, S. Burazerovic, A. Onoda, Y. M. Wilson, T. R. Ward, T. Hayashi, *Angew. Chem. Int. Ed.* **2012**, *51*, 3818–3821; *Angew. Chem.* **2012**, *124*, 3884–3887.
[48] M. Sosna, D. Fapyane, E. E. Ferapontova, *J. Electroanal. Chem.* **2014**, *728*, 18–25.
[49] E. Smith, I. Collins, *Future Med. Chem.* **2015**, *7*, 159–183.
[50] Z. Li, P. Hao, L. Li, C. Y. J. Tan, X. Cheng, G. Y. J. Chen, S. K. Sze, H.-M. Shen, S. Q. Yao, *Angew. Chem. Int. Ed.* **2013**, *52*, 8551–8556; *Angew. Chem.* **2013**, *125*, 8713–8718.
[51] L. P. Conway, A. M. Jadhav, R. A. Homan, W. Li, J. S. Rubiano, R. Hawkins, R. M. Lawrence, C. G. Parker, *Chem. Sci.* **2021**, *12*, 7839–7847.
[52] M. Baureder, L. Hederstedt, *PLoS One* **2012**, *7*, e36725.
[53] L. Frankenberg, M. Brugna, L. Hederstedt, *J. Bacteriol.* **2002**, *184*, 6351–6356.
[54] V. Saillant, D. Lipuma, E. Ostyn, L. Joubert, A. Boussac, H. Guerin, G. Brandelet, P. Arnoux, D. Lechardeur, *mBio* **2021**, *12*, e03392-20.
[55] D. Wu, A. R. Mehdipour, F. Finke, H. G. Goojani, R. R. Groh, T. N. Grund, T. M. Reichhart, R. Zimmermann, S. Welsch, D. Bald, M. Shepherd, G. Hummer, S. Safarian, *bioRxiv* **2022**, https://doi.org/10.1101/2022.04.07.487047.
[56] M. Yamashita, M. Shepherd, W. I. Booth, H. Xie, V. Postis, Y. Nyathi, S. B. Tzokov, R. K. Poole, S. A. Baldwin, P. A. Bullough, *J. Biol. Chem.* **2014**, *289*, 23177–23188.
[57] M. Baureder, L. Hederstedt, *Advances in Microbial Physiology*, Academic Press, New York, **2013**, pp. 1–43.
[58] K. O. Håkansson, M. Brugna, L. Tasse, *Acta Crystallogr. Sect. D* **2004**, *60*, 1374–1380.
[59] J. C. D. M. Campos, L. C. M. Antunes, R. B. R. Ferreira, *Future Microbiol.* **2020**, *15*, 649–677.
[60] V. Normant, L. Kuhn, M. Munier, P. Hammann, G. L. A. Mislin, I. J. Schalk, *ACS Infect. Dis.* **2022**, *8*, 183–196.
[61] J. R. Otero-Asman, A. I. García-García, C. Civantos, J. M. Quesada, M. A. Llamas, *Environ. Microbiol.* **2019**, *21*, 4629–4647.
[62] R. L. Marvig, S. Damkiær, S. M. H. Khademi, T. M. Markussen, S. Molin, L. Jelsbak, *mBio* **2014**, *5*, e00966-14.
[63] C. E. Nelson, W. Huang, L. K. Brewer, A. T. Nguyen, M. A. Kane, A. Wilks, A. G. Oglesby-Sherrouse, *J. Bacteriol.* **2019**, *201*, e00754-18.
[64] A. R. Reddi, I. Hamza, *Acc. Chem. Res.* **2016**, *49*, 1104–1110.
[65] T. Schiött, M. Throne-Holst, L. Hederstedt, *J. Bacteriol.* **1997**, *179*, 4523–4529.
[66] A. Miczák, *J. Bacteriol.* **1977**, *131*, 379–381.
[67] L. Hederstedt, *Biochemistry* **2021**, *86*, 8–21.
[68] P. Wittung-Stafshede, B. G. Malmström, J. R. Winkler, H. B. Gray, *J. Phys. Chem. A* **1998**, *102*, 5599–5601.
[69] C. R. Robinson, Y. Liu, J. A. Thomson, J. M. Sturtevant, S. G. Sligar, *Biochemistry* **1997**, *36*, 16141–16146.
[70] P. Wittung-Stafshede, J. C. Lee, J. R. Winkler, H. B. Gray, *Proc. Natl. Acad. Sci. USA* **1999**, *96*, 6587–6590.
[71] H. Mi, D. Ebert, A. Muruganujan, C. Mills, L. P. Albou, T. Mushayamaha, P. D. Thomas, *Nucleic Acids Res.* **2021**, *49*, D394–D403.
[72] S. Klumpp, T. Hwa, *Curr. Opin. Biotechnol.* **2014**, *28*, 96–102.
[73] R. L. Bertrand, *J. Bacteriol.* **2019**, *201*, e00697-18.
[74] J. Jaishankar, P. Srivastava, *Front. Microbiol.* **2017**, *8*, 2000.
[75] A. G. Torres, P. Redford, R. A. Welch, S. M. Payne, *Infect. Immun.* **2001**, *69*, 6179–6185.
[76] E. C. Hagan, H. L. T. Mobley, *Mol. Microbiol.* **2009**, *71*, 79–91.
[77] C. Zaoui, J. Overhage, D. Löns, A. Zimmermann, M. Müsken, P. Bielecki, C. Pustelny, T. Becker, M. Nimtz, S. Häussler, *Mol. Microbiol.* **2012**, *83*, 536–547.
[78] A. Hutchin, C. Cordery, M. A. Walsh, J. S. Webb, I. Tews, *Microbiol. Spectrum* **2021**, *9*, e0102621.
[79] Q. Zhao, F. Fang, Y. Shan, Z. Sui, B. Zhao, Z. Liang, L. Zhang, Y. Zhang, *Anal. Chem.* **2017**, *89*, 5179–5185.
[80] R. Bruderer, O. M. Bernhardt, T. Gandhi, Y. Xuan, J. Sondermann, M. Schmidt, D. Gomez-Varela, L. Reiter, *Mol. Cell. Proteomics* **2017**, *16*, 2296–2309.
[81] C. Lenz, H. Urlaub, *Expert Rev. Proteomics* **2014**, *11*, 409–414.
[82] S. F. Altschul, W. Gish, W. Miller, E. W. Myers, D. J. Lipman, *J. Mol. Biol.* **1990**, *215*, 403–410.
[83] B. S. Conroy, J. C. Grigg, M. Kolesnikov, L. D. Morales, M. E. P. Murphy, *BioMetals* **2019**, *32*, 409–424.
[84] P. T. dos Santos, P. T. Larsen, P. Menendez-Gil, E. M. S. Lillebæk, B. H. Kallipolitis, *Front. Microbiol.* **2018**, *9*, 3090.
[85] K. Michels, A. L. Solomon, Y. Scindia, L. Sordo Vieira, Y. Goddard, S. Whitten, S. Vaulont, M. D. Burdick, C. Atkinson, R. Laubenbacher, B. Mehrad, *J. Infect. Dis.* **2022**, *225*, 1811–1821.
[86] I. Rodríguez-Arce, T. Al-Jubair, B. Euba, A. Fernández-Calvet, C. Gil-Campillo, S. Martí, S. Törnroth-Horsefield, K. Riesbeck, J. Garmendia, *Virulence* **2019**, *10*, 315–333.
[87] F. Akhter, E. Womack, J. E. Vidal, Y. Le Breton, K. S. McIver, S. Pawar, Z. Eichenbaum, *Sci. Rep.* **2020**, *10*, 15202.
[88] A. Gruss, E. Borezée-Durant, D. Lechardeur, *Advances in Microbial Physiology*, Academic Press, New York, **2012**, pp. 69–124.
[89] S. Kim, I. Kang, J. W. Lee, C. O. Jeon, S. J. Giovannoni, J. C. Cho, *Proc. Natl. Acad. Sci. USA* **2021**, *118*, e2102750118.
[90] C. Chen, T. K. Samuel, M. Krause, H. A. Dailey, I. Hamza, *J. Biol. Chem.* **2012**, *287*, 9601–9612.
[91] J. A. Vizcaíno, E. W. Deutsch, R. Wang, A. Csordas, F. Reisinger, D. Ríos, J. A. Dianes, Z. Sun, T. Farrah, N. Bandeira, P. A. Binz, I. Xenarios, M. Eisenacher, G. Mayer, L. Gatto, A. Campos, R. J. Chalkley, H. J. Kraus, J. P. Albar, S. Martinez-Bartolomé, R. Apweiler, G. S. Omenn, L. Martens, A. R. Jones, H. Hermjakob, *Nat. Biotechnol.* **2014**, *32*, 223–226.
[92] Y. Perez-Riverol, A. Csordas, J. Bai, M. Bernal-Llinares, S. Hewapathirana, D. J. Kundu, A. Inuganti, J. Griss, G. Mayer, M. Eisenacher, E. Pérez, J. Uszkoreit, J. Pfeuffer, T. Sachsenberg, Ş. Yilmaz, S. Tiwary, J. Cox, E. Audain, M. Walzer, A. F. Jarnuczak, T. Ternent, A. Brazma, J. A. Vizcaíno, *Nucleic Acids Res.* **2019**, *47*, D442–D450.

Manuscript received: August 16, 2022
Accepted manuscript online: December 10, 2022
Version of record online: January 23, 2023